Journal of Power Sources 236 (2013) 259–264

Contents lists available at SciVerse ScienceDirect

Journal of Power Sources

journal homepage: www.elsevier.com/locate/jpowsour

Short communication

A polyoxometalate flow battery

Harry D. Pratt III [a], Nicholas S. Hudak [a], Xikui Fang [b], Travis M. Anderson [a,*]

[a] Sandia National Laboratories, Albuquerque, NM 87185, USA
[b] Ames Laboratory, Ames, IA 50011, USA

HIGHLIGHTS

- Construction of a flow battery with vanadium- and tungsten-polyoxometalates.
- Coulombic efficiencies were greater than 95% with low capacity fading.
- The compounds are stable over a wide range of conditions.
- Polyoxometalates undergo multi-electron reactions.

ARTICLE INFO

Article history:
Received 16 January 2013
Received in revised form
15 February 2013
Accepted 20 February 2013
Available online 5 March 2013

Keywords:
Flow battery
Polyoxometalates
Vanadium
Tungsten

ABSTRACT

A redox flow battery utilizing two, three-electron polyoxometalate redox couples ($SiV^{V}_{3}W^{VI}_{9}O^{7-}_{40}$/$SiV^{IV}_{3}W^{VI}_{9}O^{10-}_{40}$ and $SiV^{IV}_{3}W^{VI}_{9}O^{10-}_{40}$/$SiV^{IV}_{3}W^{V}_{3}W^{VI}_{6}O^{13-}_{40}$) was investigated for use in stationary storage in either aqueous or non-aqueous conditions. The aqueous battery had coulombic efficiencies greater than 95% with relatively low capacity fading over 100 cycles. Infrared studies showed there was no decomposition of the compound under these conditions. The non-aqueous analog had a higher operating voltage but at the expense of coulombic efficiency. The spontaneous formation of these clusters by self-assembly facilitates recovery of the battery after being subjected to reversed polarity. Polyoxometalates offer a new approach to stationary storage materials because they are capable of undergoing multi-electron reactions and are stable over a wide range of pH values and temperatures.

Published by Elsevier B.V.

1. Introduction

Global energy consumption is projected to increase at least twofold by mid-century, and this increased need will be met, at least in part, through the use of renewable energy sources. [1] Due to the intermittent nature of these resources, large-scale energy storage devices must likewise be invented, developed, and deployed in this timeframe in order for these carbon neutral technologies to be fully utilized. [2] The need for grid storage is also being driven by the evolving nature of the grid (smart grid, green grid, and the distributed nature of the grid) as well as by other technological developments, such as vehicle electrification. [3] Redox flow batteries (RFBs) are rechargeable systems that can be designed to address these issues and that can be readily scaled to meet the varied grid needs [4–8]. In these systems, the storage medium (electrolyte and dissolved charge storage species) flows through an electrochemical cell that converts between electrical energy and chemical potential (Fig. 1). However, the practical use of RFBs is limited by low energy densities. As part of our efforts to identify higher energy density storage materials for RFBs, we have now evaluated the use of early transition metal oxide clusters (commonly referred to as polyoxometalates) in a laboratory-scale flow cell.

Polyoxometalates (POMs) are a large and structurally diverse class of compounds formed by the linkage of d^0 metal-centered polyhedra with oxygen atoms located at the vertices [9–11]. The versatility and accessibility of POMs have led to many applications [12,13]. In addition, these compounds are ideal for energy storage because of their ability to undergo highly reversible multi-electron redox processes [14]. A tungsten-based Keggin structure (α-$H_4SiW_{12}O_{40}$ (**1**)) was selected for study after a stability screening because it could be prepared in high yield and high purity from relatively low-cost precursors [15]. This compound was subsequently modified to replace three corner-sharing tungsten atoms with vanadium (Fig. 1). The resulting compound, A-α-$K_6HSiV_3W_{12}O_{40}$ (**2**) [16,17] (where the charge compensating protons of **1** were mostly exchanged for potassium as part of the literature synthesis protocol), is stable over

* Corresponding author. Tel.: +1 505 844 4766; fax: +1 505 844 6972.
E-mail address: tmander@sandia.gov (T.M. Anderson).

0378-7753/$ – see front matter Published by Elsevier B.V.
http://dx.doi.org/10.1016/j.jpowsour.2013.02.056

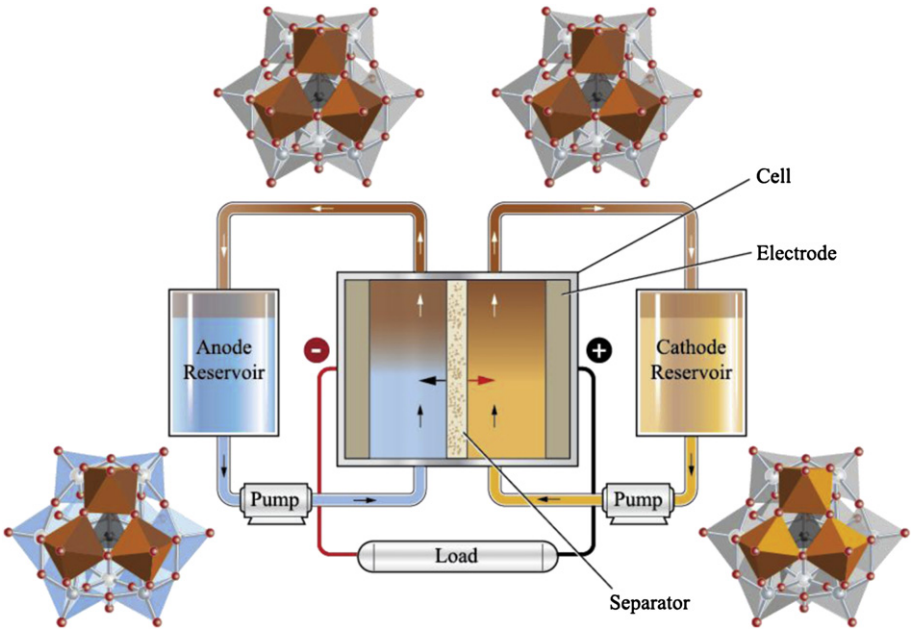

Fig. 1. Schematic of a POM RFB during discharge. The POMs are drawn in combination polyhedral/ball-and-stick notation. The orange and brown polyhedra represent oxidized and reduced vanadium, respectively, and the gray and blue polyhedra represent oxidized and reduced tungsten, respectively. The black tetrahedron represents SiO_4. (For interpretation of the references to color in this figure legend, the reader is referred to the web version of this article.)

a wide range of temperatures and pH values [18], and the electrochemistry of the vanadium centers is separated from tungsten by about 1 V. The latter property allows the same material to serve as both the cathode and anode, and it is conceptually similar to the well known all-vanadium RFB [19]. The results presented here show that utilizing the vanadium and tungsten centers of **2** as cathode and anode, respectively, yields an aqueous 0.8 V battery that could be cycled 100 times with greater than 95% coulombic efficiency (discharge capacity divided by charge capacity).

2. Experimental

2.1. Synthesis and characterization

The compounds were prepared and purified by literature methods [18]. The stability of the compounds was monitored using a Thermo Nicolet iS10 FT-IR equipped with a Smart Orbit (Diamond) ATR accessory, Thermo Scientific Evolution 220 UV–Visible Spectrophotometer, and a Bruker AXS SMART-CCD diffractometer with graphite monochromated Mo K_α (0.71073 Å) radiation. Cyclic voltammetry (CV) experiments were performed at room temperature under Ar (blanketed for aqueous electrochemistry and in an Argon glove box for non-aqueous electrochemistry) using a BASi Epsilon potentiostat. The working electrode was a freshly polished 3 mm diameter glassy carbon and the counter electrode was a Pt wire. In order to compare the aqueous *versus* non-aqueous data, we calculated the Ag/AgCl in 3 M NaCl reference electrode (BASi, nominally −35 mV *versus* a saturated calomel electrode) [20], to be 3.2 V *versus* Li/Li^+ [21], and a plot of the aqueous data referenced to Li/Li^+ is shown in the Supporting information. The reference electrode for non-aqueous experiments was Ag/AgCl in a solution of 1-ethyl-3-methyl-imidazolium chloride dissolved in 1,2-dimethyl-3-propyl-imidazolium bis(trifluoromethylsulfonyl) imide. This non-aqueous reference electrode was measured to be 2.4 V *versus* Li/Li^+ by measuring its potential *versus* a lithium-coated copper electrode in 1-butyl-3-methyl-imidazolium hexafluorophosphate containing 0.5 M $LiPF_6$.

2.2. Static cell study

An H-type cell (Adams and Chittenden Scientific Glass) with two 15 mL electrolyte compartments was used for charge–discharge experiments. The solutions in each compartment were stirred using a Teflon coated magnetic stir bar. The galvanostatic measurements were performed on a Solartron SI 1287 potentiostat under constant current conditions. The electrolytes were separated using a Nafion 117 membrane with an active area of 1 cm^2. Prior to use, the membranes were soaked in their respective test solutions overnight. Two (active area 2 cm^2) graphite electrodes (Poco) were used for charge–discharge purposes. Aqueous experiments were performed in air, and non-aqueous experiments were performed in an Argon glove box. All static cell experiments were performed at room temperature.

2.3. Flow cell study

The flow cells consisted of two carbon-felt electrodes, two graphite current collectors with machined serpentine or circular flow fields (Fuel Cell Technologies), two gaskets, and a Nafion 117 membrane. The carbon felt (GFD grade from SGL carbon, 2.5 mm nominal thickness) was treated under O_2 plasma for 5 min on each side using the Harrick Plasma cleaner (model PDC-001). The active area of the electrode for both the serpentine and circular configurations was 5 cm^2. The system includes a single cell, two peristaltic pumps (Masterflex L/S), two polypropylene reservoirs, and Viton tubing. A Solartron 1287 potentiostat was used to control the charging and discharging of the electrolytes. All flow cell experiments were performed at room temperature.

3. Results and discussion

3.1. Cyclic voltammetry

Cyclic voltammetry (CV) was first performed on **1** and **2** in order to investigate their electrochemical reversibility and kinetics in an

aqueous H_2SO_4 environment (Fig. 2A). The concentration of **1** was kept at 10 mM to allow for examination of the thermodynamics and transport under approximately diffusion controlled conditions. A common feature in the CVs of POMs is the presence of several reversible diffusion-controlled waves [14,22]. The CV of **1** using a glassy carbon (working) electrode at ambient temperature (with a scan rate of 50 mV s^{-1}) showed two reversible one-electron waves, evidenced by the 59-mV peak separations, and one reversible two-electron process, evidenced by the 30-mV peak separation, with no redox activity at higher potentials. All of the waves were attributed to the reduction and re-oxidation of the W(VI) centers present in the molecule [22]. A CV of the tri-vanadium substituted analog **2** is also shown in Fig. 2A. The three pairs of tungsten-based waves observed in **1** have now become two, two-electron processes between 0.4 V and 0.7 V (*versus* SHE). This was confirmed by bulk electrolysis measurements performed at 0.3 V (*versus* SHE), and it is consistent with the literature [23–25]. The small wave at 0.8 V (*versus* SHE) was attributed to the pH-dependent desorption of the highly charged POM from the electrode surface [25]. There were also two redox pairs between 1.3 V and 1.7 V (*versus* SHE) that were assigned to the vanadium-based processes. Bulk electrolysis performed at 1.2 V (*versus* SHE) indicated that what appears to be two peak-pairs was attributable to a total of three electrons. A square-wave voltammogram indicated that the wave centered at 1.5 V (*versus* SHE) was actually two poorly resolved redox pairs. Previous EPR studies on the lower symmetry vanadium-substituted POMs (such as **2**) showed that the waves between 1.3 V and 1.7 V (*versus* SHE) were primarily centered around the vanadium sites while those between 0.4 V and 0.7 V (*versus* SHE) were tungsten centered [26,27]. The peak separations for the two pairs of vanadium-based redox processes were 63 (one-electron) and 85 mV (two-electron), while the separations for the two pairs of two-electron tungsten-based processes were 68 and 40 mV, suggesting that these redox couples may have sufficient reversibility to be used as active materials for a RFB.

Cyclic voltammetry was also performed on a non-aqueous analog of **2** that was prepared by cation metathesis (i.e. potassium was exchanged for tetra-*n*-butylammonium to render it soluble). The resulting compound, $((CH_3CH_2CH_2CH_2)_4N)_4H_3SiV_3W_9O_{40}$ (**3**) [18], was soluble in a wide range of solvents including acetonitrile, propylene carbonate, and methanol. The non-aqueous POM **3** is considerably more difficult to reduce than its aqueous analog **2** [28]. As shown in Fig. 2B, **3** in propylene carbonate containing 0.5 M TBAOTf (where TBAOTf is $(CH_3CH_2CH_2CH_2)_4N(CF_3SO_3)$) has two pairs of waves between 2.5 V and 3.0 V (*versus* Li/Li^+), which are associated with the vanadium electrochemistry, and three poorly resolved pairs of waves between 0.2 V and 0.8 V (*versus* Li/Li^+), which are associated with quasi-reversible tungsten electrochemistry. The irreversible reduction of tungsten is observed at 0 V (*versus* Li/Li^+). The separation between the vanadium and tungsten electrochemistry was about 1.7 V (compare to about 0.8 V in the aqueous system). There is considerable interest in the use of non-aqueous electrolytes for RFBs because of the promise of wider voltage windows, enhanced temperature stability range, and higher energy and power densities [29].

3.2. Static cell studies

The charge–discharge characteristics of the POMs were first investigated at room temperature in a static cell (a cell with stagnant liquid) comprised of two 15 mL compartments separated by a Nafion 117 membrane with an active area of 1 cm^2. The stabilities of the oxidized and reduced POMs were rigorously monitored at all times by infrared and UV–Visible spectroscopy as well as ^{29}Si and ^{51}V NMR (oxidized species only) [30,31]. In addition, the cells were rigorously deoxygenated to minimize the O_2-based re-oxidation of the highly reduced complexes. Galvanostatic cycling performed on a static cell containing 20 mM **2** and 0.5 M H_2SO_4 (as the supporting electrolyte) yielded a relatively large difference between charge voltage and discharge voltage (approximately 1 V). This was likely due to significant ohmic losses resulting from the low POM concentration (mass transport limitation), small membrane area (1 cm^2) and the large distance (2 cm) between the electrodes. The low electrode surface area of the graphite plates and the lack of solution convection may have also contributed to the large cell overpotentials. The coulombic efficiency leveled out at 96% after the second cycle. The non-aqueous analog was also tested in a static cell containing 20 mM **3** and 0.5 M TBAOTf in propylene carbonate. In contrast to **2**, the coulombic efficiency of **3** continually decreased with each cycle.

Bulk electrolysis measurements (all with greater than 99% yield) on **2** and **3** show that each side of the cell underwent three-electron and two-electron transfer, respectively, during cycling. In the case of **2**, this means the cathode (positive electrode) cycled between $SiV^V_3W^{VI}_9O_{40}^{7-}$ (fully charged) and $SiV^{IV}_3W^{VI}_9O_{40}^{10-}$ (fully discharged), and the anode (negative electrode) cycled between $SiV^{IV}_3W^V_3W^{VI}_6O_{40}^{13-}$ (fully charged) and $SiV^{IV}_3W^{VI}_9O_{40}^{10-}$ (fully discharged). Prior to the assembly of the cell, bulk electrolysis was also used to generate $SiV^{IV}_3W^V_3W^{VI}_6O_{40}^{13-}$ for the anode. Thus the cell was fully charged at the beginning of each cycling experiment. To

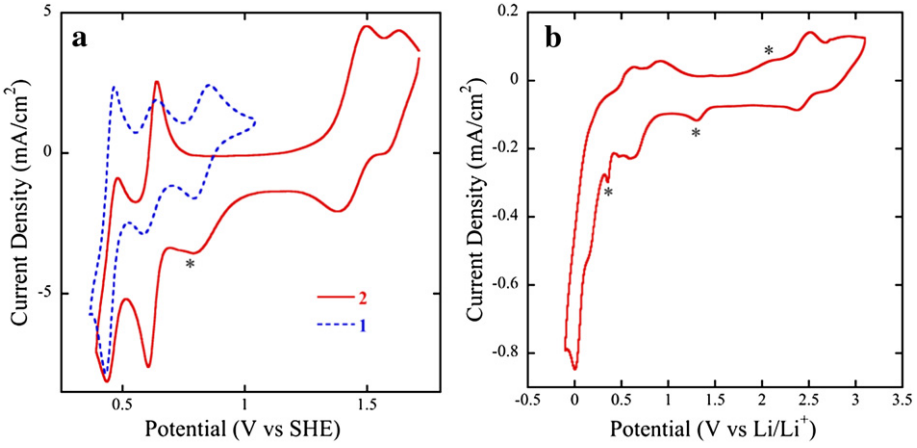

Fig. 2. (a) CV of **2** in comparison with its parent compound **1** in 0.5 M H_2SO_4 (as supporting electrolyte) using a glassy carbon working electrode with a scan rate of 50 mV s^{-1} (b) CV of **3** in 0.5 M TBAOTf in propylene carbonate using a glassy carbon working electrode with a scan rate of 50 mV s^{-1}. The peaks marked with an asterisk are attributable to the supporting electrolyte.

the best of our knowledge, a three-electron system in each individual half-cell is unprecedented in flow battery chemistry. In addition, the use of compounds capable of undergoing two or more redox processes allows for more energy storage using less material, as exemplified by the zinc-bromine RFB [4–7].

3.3. Flow cell studies

The performance of **2** (20 mM) in 0.5 M H_2SO_4 (as supporting electrolyte) was tested at room temperature by cycling it 100 times in a laboratory-scale flow cell with serpentine flow fields, carbon felt electrodes, and a Nafion 117 membrane. Galvanostatic cycling was performed at 2 mA cm^{-2} with 0.05 V and 1.4 V as voltage limits. Fig. 3A shows the voltage profile for the 2nd and 100th cycle. The capacity of the first charge plateau almost doubled from the 2nd to the 100th cycle (with a concurrent voltage increase) while that of the second charge plateau partially diminished. The voltage efficiencies for the first and second plateaus in the 100th cycle were approximately 99% and 30%, respectively. As shown in Fig. 3B, the overall coulombic efficiency was greater than 95% with less than 2% loss over 100 cycles, and the charge capacity decreased by about 10% over the same period. Cell performance can also be characterized with the "electrochemical yield", which is defined here as the observed capacity during charge or discharge divided by the theoretical capacity. Theoretical capacity is calculated using the solution concentration, solution volume, and the number of electrons transferred per molecule of active material. The electrochemical yield of the flow cell containing **2** decreased from 90% to 80% during the first 100 cycles.

After cycling, spent solutions from the flow cell were examined by UV–Visible, infrared (Fig. 4), and NMR spectroscopy (^{29}Si and ^{51}V), and there was no evidence for the decomposition of **2**. In addition, single crystal X-ray diffraction was performed upon concentrating the solution, and the results clearly show the Keggin structure was fully intact. After 100 cycles, flow cell performance was fully restored by placing the cycled solution in a fresh cell with a new membrane. This suggests that the observed capacity losses were not due to the POM. Upon reducing the discharge rate by half in a fresh cell, only one plateau is observed in both the charge and discharge states with a voltage efficiency of approximately 75%. In general, we observed that discharging **2** is more difficult than charging. The observation of different kinetics for the oxidation and reduction of POMs is well known in the literature and was found to be highly system specific [11]. In addition, the reduced forms of **2** have higher charge densities that will clearly influence their stability and reactivity.

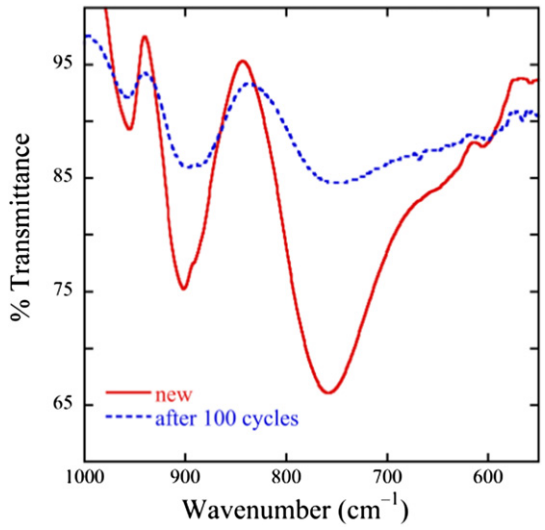

Fig. 4. FT-IR of pre (solid, red line) and post cycling (dotted, blue line). The intensity difference is due to hydration state. Specifically, the pre cycling sample was collected on a dehydrated crystalline sample of **2** while the post cycling sample was collected on a sample obtained by evaporation of the battery solution. (For interpretation of the references to color in this figure legend, the reader is referred to the web version of this article.)

Iterations of the RFB prototype were conducted in order to improve performance and better understand the potential utility of POMs in RFBs. The performance of **2** in 0.5 M H_2SO_4 (as supporting electrolyte) was also tested in a circular flow field under conditions otherwise identical to those described above. While the coulombic efficiency was maintained, there was a significant drop in the electrochemical yield (from 91% to 38%). The circular cell was of interest because it was expected to accommodate higher viscosity fluids including non-aqueous solvents and ionic liquids. Additionally, the circular cell was placed under an abusive electrochemical condition (reversed polarity) to test the robustness of the POM. After the cell reached its lower voltage limit of 50 mV, the discharge current was applied for an additional 48 h, which lowered the cell voltage to about −2 V. Upon subsequent charge, the system recovered after one cycle with slightly lower coulombic efficiency (less than 10% change) but 20% higher electrochemical yield. This observation was consistent with the fact that not only do POMs form by self-assembly, [9] but they also display self-healing properties as first reported by Hill [32].

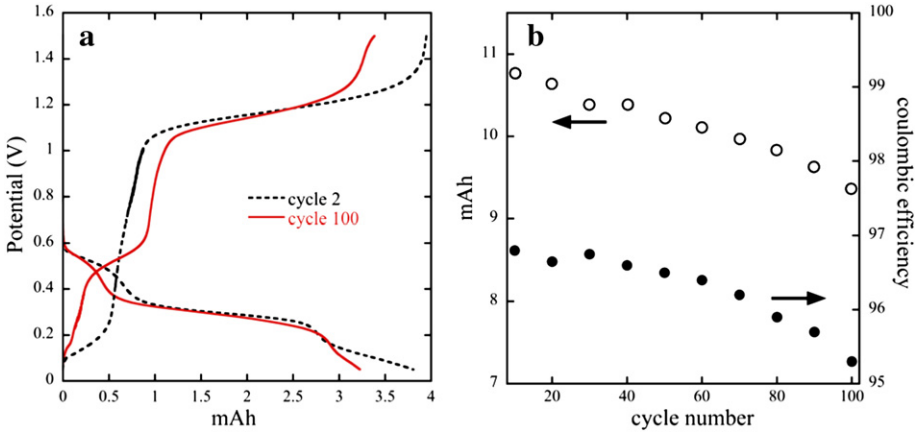

Fig. 3. (a) Voltage profiles of **2** in 0.5 M H_2SO_4 (as supporting electrolyte) in a serpentine flow cell performed at 2 mA cm^{-2} at a flow rate of 2.5 mL min^{-1}. (b) Charge capacity and coulombic efficiency of the cell from (a) as a function of cycle number.

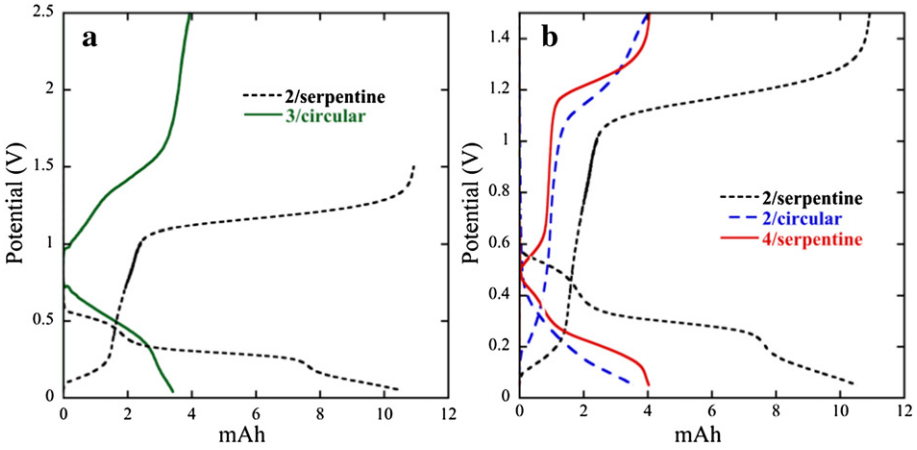

Fig. 5. (a) Voltage profiles comparing aqueous (**2** at 2 mA cm^{-2}) and non-aqueous (**3** at 0.5 mA cm^{-2}) chemistries at flow rates of 2.5 and 10 mL min^{-1}, respectively. (b) Voltage profiles comparing flow cell geometries and the influence of counter cations (all at 2 mA cm^{-2} and flow rates of 2.5 mL min^{-1} (**2**) and 5 mL min^{-1} (**4**)).

The non-aqueous analog **3** (20 mM) in 0.5 M TBAOTf in propylene carbonate was tested in a circular flow cell at 0.5 mA cm^{-2} with 0.05 V and 2.5 V as voltage limits, and the capacity curves are shown in Fig. 5A. While the initial coulombic efficiency was 87% and the open-circuit voltage was slightly improved (0.3 V higher than the aqueous system), the cycling rate and electrochemical yield were 65% and 15% lower than the aqueous flow systems of **2**. After 10 cycles, the electrochemical yield of the system dropped by half. A previous report on a non-aqueous ruthenium-based RFB suggests efficiencies can be improved with optimization of the separator and flow rate as well as by the concentration of the active material [29b].

In order to better understand the role of the cation in the performance of a POM [33] in a RFB (including electrochemical reversibility, stability, and solubility), a fully protonated analog of **2**, $H_7SiV_3W_9O_{40}$ (**4**), was prepared by use of a cation exchange resin (Rexyn 102). The limited solubility of **4** required the use of more dilute H_2SO_4 (0.25 M instead of 0.50 M) to maintain the same conditions in **2**. Although the electrochemical yield of **4** in a 0.25 M H_2SO_4 electrolyte (serpentine cell) was very low (2%) at 2.5 mL min^{-1}, it increased to 27% by doubling the flow rate. The higher flow rate did not produce a significant change in coulombic efficiency. The charge–discharge curves for this particular experiment are shown in Fig. 5B. The chemistry of **4** is quite complex due to the equilibrium between H_3O^+ counter cations (i.e. protonated water) and protonated POM structures [11]. The results suggest that the alkali cation played an important role in the performance of the POM in a RFB.

An important aspect of RFB performance is the ability to obtain the highest concentration of charge storage species possible. In POM chemistry, this is commonly controlled with the counter cations [34]. While the maximum solubility of **2** in water is 0.45 M, this can be doubled by the exchange of potassium for lithium (Dowex 50W-X8). Given that the redox processes involve three-electrons at both half-cells, this represents a potential concentration of 2.7 M, which is competitive with the well-known aqueous all-vanadium RFB [19]. Although tungsten is more expensive than vanadium, POMs can also be made with molybdenum metal centers. At present, molybdenum is considerably cheaper than either vanadium or tungsten. Efforts are now underway to optimize a higher energy density system, and the results will be reported in due course.

4. Conclusions

A POM containing vanadium and tungsten redox active centers was successfully demonstrated to store charge *via* a three-electron process in a laboratory-scale flow cell for both aqueous and non-aqueous chemistries. The aqueous battery demonstrated coulombic efficiencies greater than 95% with relatively low capacity fading over 100 cycles. In addition, the system recovered from 48 h of reversed polarity after only one cycle. The non-aqueous system had a higher operating voltage (1.1 V) but at the expense of coulombic efficiency. Although the current densities were at least one order of magnitude below those normally reported in RFBs, this may be partially alleviated by increasing the concentration of the material (assuming there are mass transport limitations). POMs represent a new approach to flow battery electrolyte stability because they are highly robust and stable over a wide range of pH values and temperatures. In addition, the concentrations of acid electrolyte that were required to maintain stability were lower than those in the all-vanadium RFB, resulting in potentially less corrosion on system components and a better environmental footprint. Finally, a quick search on the term “polyoxometalates” yielded almost 20,000 references (with approximately 5,000 of them based on the Keggin structure alone), suggesting that the wealth of knowledge on POMs might be utilized to advance this technology further.

Acknowledgments

We thank the Sandia National Laboratories’ LDRD program for funding the synthesis, characterization, and static cell testing and the U. S. Department of Energy, Office of Electricity Delivery and Energy Reliability (Dr. Imre Gyuk, Energy Storage Program), for funding the flow cell testing, and Jonathan Leonard, David Ingersoll, Chris Brigman, and Chad Staiger for technical assistance. We also thank Professor Ulrich Kortz for providing a titanium-substituted POM for screening. Sandia National Laboratories is a multi-program laboratory operated by Sandia Corporation, a wholly owned subsidiary of Lockheed Martin company, for the U. S. Department of Energy’s National Nuclear Security Administration under contract DE-AC04-94AL85000. The work at Ames Laboratory (magnetic measurements and assistance with synthesis) was supported by the Department of Energy-Basic Energy Sciences under Contract No. DE-AC02-07CH11358.

Appendix A. Supplementary data

Supplementary data related to this article can be found at http://dx.doi.org/10.1016/j.jpowsour.2013.02.056.

References

[1] C. Wadia, P. Albertus, V. Srinivasan, J. Power Sources 196 (2011) 1593.
[2] J. Liu, J.-G. Zhang, Z. Yang, J.P. Lemmon, C. Imhoff, G.L. Graff, L. Li, J. Hu, C. Wang, J. Xiao, G. Xia, V.V. Viswanathan, S. Baskaran, V. Sprenkle, X. Li, Y. Shao, B. Schwenzer, Adv. Funct. Mater. 23 (2013) 929.
[3] Z. Yang, J. Zhang, M.C. Kintner-Meyer, X. Lu, D. Choi, J.P. Lemmon, J. Liu, Chem. Rev. 111 (2011) 3577.
[4] T. Nguyen, R.F. Savinell, Electrochem. Soc. Interface 19 (2010) 54.
[5] M. Skyllas-Kazacos, M.H. Chakrabarti, S.A. Hajimolana, F.S. Mjalli, M. Saleem, J. Electrochem. Soc. 158 (2011) R55.
[6] A.Z. Weber, M.M. Mench, J.P. Meyers, P.N. Ross, J.T. Gostick, Q. Liu, J. Appl. Electrochem. 41 (2011) 1137.
[7] W. Wang, Q. Luo, B. Li, X. Wei, L. Li, Z. Yang, Adv. Funct. Mater. 23 (2013) 970.
[8] P. Leung, X. Li, C. Ponce de León, L. Berlouis, C.T.J. Low, F.C. Walsh, RSC Adv. 2 (2012) 10125.
[9] M.T. Pope, A. Müller, Angew. Chem. Int. Ed. 30 (1991) 34.
[10] M.T. Pope, Polyoxo Anions: Synthesis and Structure, in: A.G. Wedd (Ed.), Comprehensive Coordination Chemistry II: From Biology to Nanotechnology, Elsevier Ltd., Oxford, UK Oxford, 2003, pp. 635–678.
[11] C.L. Hill, Polyoxometalates: Reactivity, in: A.G. Wedd (Ed.), Comprehensive Coordination Chemistry-II: From Biology to Nanotechnology, Elsevier, Oxford, 2003, pp. 679–759.
[12] D.E. Katsoulis, Chem. Rev. 98 (1998) 359.
[13] Recently, POMs have been developed for lithium battery technologies. For example, see (a) N. Kawasaki, H. Wang, R. Nakanishi, S. Hamanaka, R. Kitaura, H. Shinohara, T. Yokoyama, H. Yoshikawa, K. Awaga, Angew. Chem. Int. Ed. 50 (2011) 3471;
(b) H. Wang, S. Hamanaka, Y. Nishimoto, S. Irle, T. Yokoyama, H. Yoshikawa, K. Awaga, J. Am. Chem. Soc. 134 (2012) 4918.
[14] M.T. Pope, Heteropoly and Isopoly Oxometalates, Springer-Verlag, Berlin, 1983.
[15] A. Tézé, G. Hervé, α-, β-, and γ-Dodecatungstosilicic Acids: Isomers and Related Lacunary Compounds, in: A.P. Ginsberg (Ed.), Inorganic Syntheses, John Wiley and Sons, New York, 1990, pp. 85–96.
[16] The tri-vanadium-substituted Keggin structures are noted as A-type for three corner-sharing vanadium sites and B-type for three edge-sharing vanadium sites. The α notation refers to the most stable (generally) Baker-Figgis W_3O_{13} cap rotation isomer. For more information, see Ref. [17]. A phosphorus analog of **2**, A-α-$K_6PV_3W_9O_{40}$, was also screened in this work, but optimal stability conditions have not yet been identified.
[17] L.C.W. Baker, J.S. Figgis, J. Am. Chem. Soc. 92 (1970) 3794.
[18] R.G. Finke, B. Rapko, R.J. Saxton, P.J. Domaille, J. Am. Chem. Soc. 108 (1986) 2947.
[19] Representative, recent VRB publications include: (a) M. Vijayakumar, S.D. Burton, C. Huang, L. Li, Z. Yang, G.L. Graff, J. Liu, J. Hu, M. Skyllas-Kazacos, J. Power Sources 195 (2010) 7709;
(b) L. Li, S. Kim, W. Wang, M. Vijayakumar, Z. Nie, B. Chen, J. Zhang, G. Xia, J. Hu, G. Graff, J. Liu, Z. Yang, Adv. Energy Mater. 1 (2011) 394;
(c) X.W. Wu, T. Yamamura, S. Ohta, Q.X. Zhang, F.C. Lv, C.M. Liu, K. Shirasaki, I. Satoh, T. Shikama, D. Lu, S.Q. Liu, J. Appl. Electrochem. 41 (2011) 1183;
(d) J. Zhang, L. Li, Z. Nie, B. Chen, M. Vijayakumar, S. Kim, W. Wang, B. Schwenzer, J. Liu, Z. Yang, J. Appl. Electrochem. 41 (2011) 1215;
(e) Q.H. Liu, G.M. Grim, A.B. Papandrew, A. Turhan, T.A. Zawodzinski, M.M. Mench, J. Electrochem. Soc. 159 (2012) A1246;
(f) A. Tang, S. Ting, J. Bao, M. Skyllas-Kazacos, J. Power Sources 203 (2012) 165;
(g) D.S. Aaron, Q. Liu, G.M. Grim, A.B. Papandrew, A. Turhan, T.A. Zawodzinski, M.M. Mench, J. Power Sources 206 (2012) 450;
(h) K.J. Kim, M.-S. Park, J.-H. Kim, U. Hwang, N.J. Lee, G. Jeong, Y.-J. Kim, Chem. Commun. 48 (2012) 5455.
[20] http://www.basinc.com/products/ec/faqele.html.
[21] A.J. Bard, L.R. Faulkner, Electrochemical Methods: Fundamental and Applications, second ed., John Wiley and Sons, Inc., New York, 2001.
[22] B. Keita, L. Nadjo, Electrochemistry of Isopoly and Heteropoly Oxometalates, in: A.J. Bard, M. Stratmann (Eds.), Encyclopedia of Electrochemistry, Wiley-VCH, Weinheim, 2006, pp. 607–700.
[23] D.P. Smith, M.T. Pope, Inorg. Chem. 12 (1973) 331.
[24] E. Cadot, M. Fournier, A. Tézé, G. Hervé, Inorg. Chem. 35 (1996) 282.
[25] C. Li, Y. Zhang, K.P. O'Halloran, J. Zhang, H. Ma, J. Appl. Electrochem. 39 (2009) 421.
[26] J. Altenau, M.T. Pope, R.A. Prados, H. So, Inorg. Chem. 14 (1975) 417.
[27] M.M. Mossoba, C.J. O'Connor, M.T. Pope, E. Sinn, G. Hervé, A. Tézé, J. Am. Chem. Soc. 102 (1980) 6864.
[28] S.P. Harmalker, M.T. Pope, Inorg. Biochem. 28 (1986) 85.
[29] Representative publications include: (a) M. Morita, Y. Tanaka, K. Tanaka, Y. Matsuda, T. Matsumura-Inoue, Bull. Chem. Soc. Jpn. 61 (1988) 2711;
(b) Y. Matsuda, K. Tanaka, M. Okada, Y. Takasu, M. Morita, J. Appl. Electrochem. 18 (1988) 909;
(c) Q. Liu, A.E.S. Sleightholme, A.A. Shinkle, Y. Li, L.T. Thompson, Electrochem. Commun. 11 (2009) 2312;
(d) Q. Liu, A.A. Shinkle, Y. Li, C.W. Monroe, L.T. Thompson, A.E.S. Sleightholme, Electrochem. Commun. 12 (2010) 1634;
(e) J.-H. Kim, K.J. Kim, M.-S. Park, N.J. Lee, U. Hwang, H. Kim, Y.-J. Kim, Electrochem. Commun. 13 (2011) 997;
(f) M. Dudata, B. Ho, V.C. Wood, P. Limthongkul, V.E. Brunini, W.C. Carter, Y.-M. Chiang, Adv. Energy Mater. 1 (2011) 511;
(g) A.E.S. Sleightholme, A.A. Shinkle, Q. Liu, Y. Li, C.W. Monroe, L.T. Thompson, J. Power Sources 196 (2011) 5742;
(h) J. Mun, M.-J. Lee, J.-W. Park, D.-J. Oh, D.-Y. Lee, S.-G. Doo, Electrochem. Solid State 15 (2012) A80;
(i) W. Wang, W. Xu, L. Cosimbescu, D. Choi, L. Li, Z. Yang, Chem. Commun. 48 (2012) 6669.
[30] The two most stable Baker–Figgis isomers of $SiV_3W_9O_{40}^{7-}$ (α and β) were individually examined and although they have distinct cyclic voltammograms (and exist in equilibrium), they were relatively indistinguishable for cell charging and discharging purposes. For more information on POM isomerization and equilibria, see Ref. [31].
[31] I.A. Weinstock, J.J. Cowan, E.M.G. Barbuzzi, H. Zeng, C.L. Hill, J. Am. Chem. Soc. 121 (1999) 4608.
[32] C.L. Hill, X. Zhang, Nature 373 (1995) 324.
[33] M.-H. Chiang, J.A. Dzielawa, M.L. Dietz, M.R. Antonio, J. Electroanal. Chem. 567 (2004) 77.
[34] T.L. Jorris, M. Kozik, N. Casañ-Pastor, P.J. Domaille, R.G. Finke, W.K. Miller, L.C.W. Baker, J. Am. Chem. Soc. 109 (1987) 7402.